Anthrylmethylamines and anthrylmethylazamacrocycles as fluorescent pH sensors—a systematic study of their static and dynamic properties

Gerhard Greiner * and Ingrid Maier

Institut für Chemie, Fachgebiet Physikalische Chemie, Universität Hohenheim, 70593 Stuttgart, Germany. E-mail: greiner@uni-hohenheim.de; Fax: +7114593881

Received (in Cambridge, UK) 14th November 2001, Accepted 5th March 2002
First published as an Advance Article on the web 27th March 2002

The pH dependent fluorescence of various 9-mono- and 9,10-disubstituded anthracenes is reported. They have a compartmental structure: fluorophore (anthracene)–spacer (methylene)–and ionophore (mono-, polyamines, azamacrocycles). In these *n*-basic anthrylmethylamines the fluorescence of anthracene is intramolecularly quenched by unprotonated amine groups. The pK_A values have been evaluated by titration in order to calculate the amount (mole fraction) of each of the $n + 1$ differently charged species and their dependence on the pH. The fluorescence–pH profiles (intensities and lifetime *versus* pH) have been determined, and interpreted as the formation of differently protonated species with different fluorescence intensities and hence different fluorescence lifetimes. The experimentally determined fluorescence lifetime–pH profiles can be described by three lifetimes. This is corroborated by global analysis. The measurement of the fluorescence quantum yields of the completely protonated species yielded the radiative lifetimes. The rate constants and quantum yields of the photoinduced electron transfer (PET) are calculated for the species with shorter lifetimes and hence smaller fluorescence intensities.

Introduction

Anthrylmethylamines and anthrylmethylazamacrocycles are compounds which can be used as pH dependent chemosensors: the fluorescence of anthracene in these compounds is quenched by intramolecular photoinduced electron transfer (PET) from the lone electron pair of the nitrogen to the anthracene moiety. Protonation of the amine groups[1] or, instead of this, chelation by metal ions in the case of the anthrylmethylazamacrocycles[2] prevents the electron transfer, and thus enhances the fluorescence intensity. Because of the compartmental structure fluorophore–spacer–ionophore a wide variety of chemosensors is accessible,[1d] the properties of which can be predicted to a great extent from its components.[1b,2d,3]

Anthrylmethylamines containing more than one amine group can be protonated at different amine groups, depending on their pK_A values and the pH (Fig. 5). The pH dependent equilibria between variously protonated species with different fluorescence intensities determine the appearance of the fluorescence–pH profiles (fluorescence intensity *versus* pH). To gain a deeper insight into these pH dependent equilibria, we combined pH dependent fluorescence intensities and fluorescence lifetimes with the results of titration.

The following series of 16 different 9-mono or 9,10-disubstituted anthracenes was provided by Professor A. W. Czarnik, then of Ohio State University. The synthesis of the azamacrocycles **14** to **16** is described in ref. 1*d*.

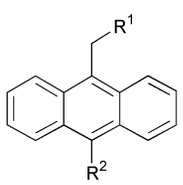

1 $R^1 = N(CH_3)_2$, $R^2 = H$
2 $R^1 = N(C_2H_5)_2$, $R^2 = H$
3 $R^1 = NH(CH_2)_2NH_2$, $R^2 = H$
4 $R^1 = [NH(CH_2)_2]_2NH_2$, $R^2 = H$
5 $R^1 = [NH(CH_2)_2]_3NH_2$, $R^2 = H$
6 $R^1 = [NH(CH_2)_2]_4NH_2$, $R^2 = H$
7 $R^1 = NH(CH_2)_3NH_2$, $R^2 = H$
8 $R^1 = NH(CH_2)_3NH(CH_2)_2NH(CH_2)_3NH_2$, $R^2 = H$
9 $R^1 = NH(CH_2)_3NH(CH_2)_4NH(CH_2)_3NH_2$, $R^2 = H$
10 $R^1 = NH(CH_2)_3N[(CH_2)_3NH_2]_2$, $R^2 = H$
11 $R^1 = NH(CH_2)_2NH_2$, $R^2 = CH_2R^1$
12 $R^1 = NH(CH_2)_3NH_2$, $R^2 = CH_2R^1$
13 $R^1 = [NH(CH_2)_2]_2NH_2$, $R^2 = CH_2R^1$

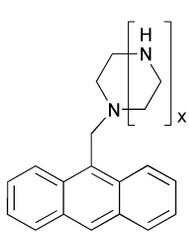

14 x = 1
15 x = 2
16 x = 4

Results

pK_A values

The general equation of pH dependent equilibria of the protonated *n*-basic anthrylmethylamines in aqueous solution is given by:

$$H_{n-i+1}A^{(n-i+1)+} + H_2O \rightleftharpoons H_{n-i}A^{(n-i)+} + H_3O^+ \ (i = 1, 2, \ldots n) \quad (1)$$

The pK_A values of the monoamines **1** and **2** were determined by fluorimetric titration, *i.e.* from the fluorescence intensities as the points of intersection with the pH axis in the linear plots of the expression $\lg [(I_{max} - I_{min})/(I - I_{min}) - 1]$ *versus* pH (ref. 1*b*,

Table 1 pK_A values in aqueous solution at room temperature

	pK_A values
1	8.6
2	9.4
3	6.1, 9.4
4	4.0, 7.7, 9.4
5	3.2, 5.8, 8.4, 9.6
6	2.7, 4.2, 6.8, 8.4, 9.4
7	7.3, 10.1
8	5.1, 7.1, 8.8, 10.0
9	6.7, 8.2, 9.8, 10.8
10	5.7, 7.9, 9.1, 10.1
11	4.6, 6.0, 9.0, 9.9
12	6.2, 7.5, 9.7, 10.4
13	2.0, 3.5, 6.5, 8.1, 9.3, 10.3
14	3.6, 9.0
15	1.8, 5.0, 10.2

Henderson–Hasselbalch-type mass action equation). This holds, as the protonation and deprotonation reactions in the excited state are negligibly slow compared to the fluorescence decay rate constants and the acidic and basic species absorb equally strongly. In this case, the amounts (mole fractions) in the excited state are the reflection (mirror image) of the amounts in the electronic ground state.[1a,f,4] In addition, the pK_A values of both electronic states are essentially identical, as the fluorophore anthracene is separated from the ionophore amine by the methylene spacer (predictability from the components).

The pK_A values of the di- and polyamines **3** to **15** were determined by potentiometric titration, *i.e.* from a plot of pH *versus* the amount of added NaOH, normalized to the degree of titration, τ.[5] Due to low concentrations (*e.g.* because of low solubility of some of the unprotonated anthrylmethylamines) and the existence of several points of inflection, the classical methods of the graphical determination of the pK_A values are inexact.[5] The results can be improved by calculating the degree of titration τ at various pH values, adapting the pK_A values for an optimal fit of the simulated and the experimental curve:

$$\tau = \frac{10^{-pK_W+pH} - 10^{-pH}}{C_0(H_nA^{n+})} + \frac{\sum_{i=0}^{n}\left[i10^{(n-i)(-pH)+\sum_{j=1}^{i}-pK_{Aj}} \right]}{\sum_{i=0}^{n}\left[10^{(n-i)(-pH)+\sum_{j=1}^{i}-pK_{Aj}} \right]} \quad (2)$$

Under the experimental conditions, a correction for the increase in volume during titration is not necessary.

All pK_A values are compiled in Table 1. For pentaazamacrocycle **16**, the pK_A values could not be determined because of lack of sufficient substance.

Fluorescence lifetimes, PET rate constants and PET quantum yields

Fluorescence lifetimes were determined by single photon counting (SPC). The goodness of the fit was judged by the reduced chi-squared χ^2.

At low pH values, all substances (with the exception of the anthrylmethylazamacrocycles **14** to **16**) showed monoexponential fluorescence decay with the longest lifetime $\tau_1 = \tau_{max}$. This decay can be assigned to the completely protonated species with the highest fluorescence intensity, I_{max}.

With increasing pH, the experimental SPC data could only be reconvoluted with a reasonably low χ^2 using a 3-exponential fit program (FIT 3 of IBH software, R. E. Imhof, 1989), yielding the lifetimes τ_1, τ_2 and τ_3 (Table 2). This reflects the mixture of various differently protonated species. We assign τ_2 to all species which are still protonated at the amine group closest to the anthracene moiety (but not completely protonated), and assign τ_3 to all species not protonated at this amine group.[1d,2g,h]

This was corroborated by a global analysis (FIT 12 of IBH software) of all decay curves of a substance at different pH values with a common set of lifetimes τ_1, τ_2 and τ_3 (and for some substances lifetimes τ_1', τ_2 and τ_3 for the higher pH range respectively, see fluorescence–pH profiles).

At high pH values, essentially only the unprotonated amine with its very short lifetime $\tau_3 = \tau_{min}$ and its weak fluorescence, I_{min}, can be found. As this lifetime is uncertain under the given experimental conditions, it was calculated from the relation:

$$\tau_3 = \frac{I_{min}}{I_{max}}\tau_1 \quad (3)$$

This holds, as the fluorescence intensity is proportional to the fluorescence quantum yield[1a,6] and thus, as the radiative lifetime is constant,[7] to the fluorescence lifetime. The rate constants of the intramolecular photoinduced electron transfer (k_{PET}) of the species with the lifetime τ were calculated from:

$$k_{PET} = \frac{1}{\tau} - \frac{1}{\tau_{max}} \quad (4)$$

and the quantum yields of PET (ϕ_{PET}):

$$\phi_{PET} = k_{PET}\tau = 1 - \frac{\tau}{\tau_{max}} \quad (5)$$

For the completely protonated species with the longest lifetime $\tau_1 = \tau_{max}$, $k_{PET} = 0$ and $\phi_{PET} = 0$. For some polyamines, species with the fluorescence lifetime τ_1' have to be assumed to fit the fluorescence–pH profiles. In this case, the rate constants of the fluorescence quenching PET are lower than 6×10^7 s^{-1}, and its quantum yields are at the most 0.4. For species with the intermediate fluorescence lifetime τ_2, the PET rate constants are between 1 to 3×10^8 s^{-1} and its quantum yields 0.6 to 0.8. For species with the shortest fluorescence lifetime τ_3, the rate constants and the quantum yields of the competing PET are the highest.[1d,2g,h] Two groups can be distinguished: monoamine **1** and the disubstituted anthracenes **11** to **13** with PET rate constants from 12 to 15×10^9 s^{-1} and PET quantum yields higher than 0.99, and all other amines with PET rate constants from 2 to 5×10^9 s^{-1} and PET quantum yields from 0.96 to 0.99. For the disubstituted anthracenes **11** to **13**, the higher PET rates are comprehensible, as there are two amine groups nearby the anthracene.

Fluorescence quantum yields at low pH values

The fluorescence quantum yields ϕ_f of **7**, **11** and **14** were determined relative to quinine sulfate at pH = 1. In addition, for all substances the fluorescence quantum yields corresponding to the high fluorescence intensity plateau value at low pH were determined relative to diamine **7** by integrating the emission corrected fluorescence spectra.

Given the fluorescence quantum yield ϕ_f and the fluorescence lifetime τ_1 at low pH of a substance, the radiative lifetime τ_n can be calculated:

$$\tau_n = \frac{\tau_1}{\phi_f} \quad (6)$$

These values are compiled in Table 3.

For the noncyclic amines **1** to **13**, the fluorescence quantum yields are approximately 0.6 to 0.7. For the azamacrocycles **14** to **16**, these values are significantly lower, 0.1 to 0.2.

Table 2 Fluorescence lifetimes, PET rate constants and PET quantum yields of species with τ_1', τ_2 and τ_3 in aqueous solution at room temperature

	Fluor. lifetimes/ns				$k_{PET}/10^9$ s^{-1}			ϕ_{PET} (%)		
	τ_1 [a]	τ_1' [b]	τ_2 [a]	τ_3 [b]	τ_1'	τ_2	τ_3	τ_1'	τ_2	τ_3
1	13.0	—	—	0.073	—	—	13.6	—	—	99.4
2	12.9	—	—	0.29	—	—	3.3	—	—	97.7
3	11.8	—	4.1	0.32	—	0.16	3.0	—	65	97.3
4	11.8	9.8	3.5	0.33	0.017	0.20	3.0	17	70	97.2
5	12.0	11.3	3.3	0.44	0.005	0.22	2.2	6	73	96.3
6	11.8	9.9	2.7	0.37	0.016	0.29	2.7	16	77	96.9
6			3.9 [b]			0.17			67	
7	11.7	—	3.0	0.18	—	0.25	5.4	—	74	98.5
8	11.7	—	3.6	0.21	—	0.19	4.8	—	69	98.3
9	11.7	7.0	3.9	0.19	0.057	0.17	5.3	40	67	98.4
10	11.9	—	5.1	0.24	—	0.11	4.2	—	57	98.0
11	11.8	—	4.0	0.065	—	0.17	15.3	—	66	99.5
12	11.0	—	– [d]	0.066	—	—	15.2	—	—	99.4
13	11.8	—	5.1	0.086	—	0.11	11.6	—	57	99.7
14	10.6	—	4.0	0.31	—	0.16	3.1	—	62	97.1
15	12.7	—	2.6	0.23	—	0.31	4.2	—	80	98.2
16	10.0	—	3.3	0.40 [a]	—	— [c]	— [c]	—	– [c]	— [c]

[a] Determined by SPC. [b] Calculated from $\tau = I/I_{max}\tau_1$. [c] No data, as the pK_A values are unknown. [d] Biexponential decay with τ_1 and τ_3 fits to the experimental data.

Table 3 Fluorescence quantum yields, decay times τ_1 at low pH and radiative lifetimes τ_n in aqueous solution at room temperature

	ϕ_f [a]	ϕ_f [b]	τ_1/ns	τ_n/ns
1	0.71		13.0	18.8
2	0.73		12.9	18.2
3	0.61		11.8	20.0
4	0.64		11.8	18.7
5	0.66		12.0	18.5
6	0.60		11.8	20.3
7		0.61	11.7	19.2
8	0.61		11.7	19.2
9	0.61		11.7	19.2
10	0.58		11.9	20.2
11	0.71	0.65	11.8	16.2
12	0.65		11.0	16.2
13	0.54		11.8	21.1
14	0.21	0.18	4.0 [c]	21.1
15	0.10		— [d]	— [d]
16	0.14		— [d]	— [d]

[a] Relative to diamine **7**. [b] Relative to quinine sulfate. [c] At low pH monoexponential fluorescence decay with τ_2. [d] At low pH there is no monoexponential fluorescence decay.

Amine **14** is the only azamacrocycle with a monoexponential fluorescence decay at low pH and thus only for this macrocycle can the radiative lifetime be determined. Surprisingly, the fluorescence decay time at low pH is only 4.0 ns and so a radiative lifetime similar to that of the noncyclic amines **1** to **13** results. (The longest lifetime of 10.6 ns is assigned to a monoprotonated species present only in a small fraction of the two monoprotonated species.) The range of the radiative lifetimes is 16 to 21 ns.

Fluorescence–pH profiles

As there is a red shift of about 5 nm of the completely protonated species compared to the unprotonated species, the fluorescence intensity at a fixed wavelength is not strictly proportional to the overall fluorescence intensity of a substance. Therefore, the fluorescence intensity I was determined from the integrated, emission corrected fluorescence spectrum. In buffered solutions, the normalized fluorescence intensities (I/I_{max}) of all substances varied between 100% at low pH and 0.6% (monoamine **1**) to 8% (azamacrocycle **14**) at high pH. For the azamacrocycle **16** a decrease of 40% in I/I_{max} appeared when the pH was changed from 2 to 1. This tendency was also observed for azamacrocycle **15**, with a decrease of 15%, but not in the azamacrocycle **14**.

Using the pK_A values, pK_{Aj}, the fractions $x(H_{n-i}A^{(n-i)+})$ of the $(n-i)$-fold protonated species $H_{n-i}A^{(n-i)+}$ can be calculated for any pH value:

$$x(H_{n-i}A^{(n-i)+}) = \frac{c(H_{n-i}A^{(n-i)+})}{c_0(H_nA^{n+})} = \frac{10^{(n-i)(-pH)+\sum_{j=1}^{i}-pK_{Aj}}}{\sum_{r=0}^{n}\left[10^{(n-r)(-pH)+\sum_{j=1}^{i}-pK_{Aj}}\right]} \quad (7)$$

Finally, to each of the $n+1$ differently charged species, a relative fluorescence intensity (I_{max} ... I_{min}) is assigned, so that the simulated fluorescence–pH profile calculated from:

$$I = x(H_nA^{n+})I_{max} + \sum_{i=1}^{n-1}[x(H_{n-i}A^{(n-i)+})I_{H_{n-i}A^{(n-i)+}}] + x(A)I_{min} \quad (8)$$

fits the experimental fluorescence–pH profile.

As examples, these profiles are presented for the amines **1**, **6**, **11** and **14** in Fig. 1a to 4a respectively.

It is assumed that the highest fluorescence intensitiy I_{max} is emitted by the completely protonated species and that these species have the longest fluorescence lifetime τ_1, with the PET completely inhibited (Table 4, exceptions: pentaazamacrocycles **14** to **16**). For several polyamines, the $(n-1)$-fold protonated species have the highest fluorescence intensity I_{max} and the longest fluorescence lifetime τ_1. In some cases, a fluorescence intensitiy smaller than I_{max}, but larger than that corresponding to τ_2, was observed, and assigned to a fluorescence lifetime τ_1'.

It is assumed that the intermediate fluorescence intensity is caused by the not-completely-protonated species with the amine group closest to the anthracene moiety still protonated and that these species have the intermediate fluorescence lifetime τ_2. The remaining unprotonated amine groups quench less efficiently than an unprotonated amine group next to the anthracene moiety.[1d,2g,h] For the 9,10-disubstituted anthracenes **11** to **13**, the two amine groups next to the anthracene must be protonated to inhibit their efficient quenching.[1a]

If the fluorescence intensitiy of a particular protonation step corresponds to the lifetime τ_2, it is assumed that all existing protonation isomers of this protonation step are still protonated at the amine group closest to the anthracene moiety,

Table 4 Protonation of the species with the fluorescence lifetimes τ_1, τ_1', τ_2 and τ_3 in aqueous solution at room temperature

	No. of protons per molecule				
	N^a	τ_1	τ_1'	τ_2	τ_3
1	1	1	—	—	0
2	1	1	—	—	0
3	2	2	—	1	0–1
4	3	3	2	1	0–1
5	4	4	3	2	0–1
6	5	4–5	3	2	0–1
7	2	2	—	1	0–1
8	4	3–4	—	2	0–1
9	4	4	3	2	0–2
10	4	4	—	2–3	0–2
11	4	4	—	3	0–3
12	4	3–4	—	—	0–3
13	6	5–6	—	3–4	0–4
14	2	1	—	2	0–1
15	3	2–3	—	1–3	0–1

[a] No. of amine groups per molecule.

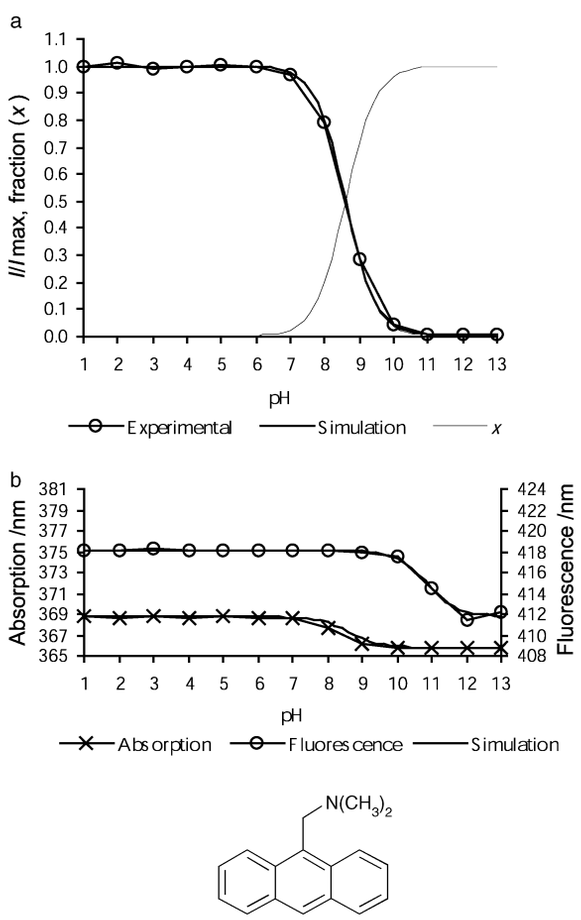

Fig. 1 Monoamine **1**, pK_A 8.6. **a** Fluorescence intensity–pH profiles and fraction–pH profiles. Numerical simulation: $I = x(HA^+) + 0.0056x(A)$. **b** Absorption maxima ($S_{0,0} \longrightarrow S_{1,1}$)–pH profiles and fluorescence maxima ($S_{1,0} \longrightarrow S_{0,1}$)–pH profiles. Numerical simulation: $\lambda_{abs} = x(HA^+) \times 368.8$ nm + $x(A) \times 365.8$ nm; $\lambda_{flu} = \{x(HA^+) \times 418.1$ nm + $0.0056x(A) \times 411.8$ nm$\}/\{x(HA^+) + 0.0056x(A)\}$.

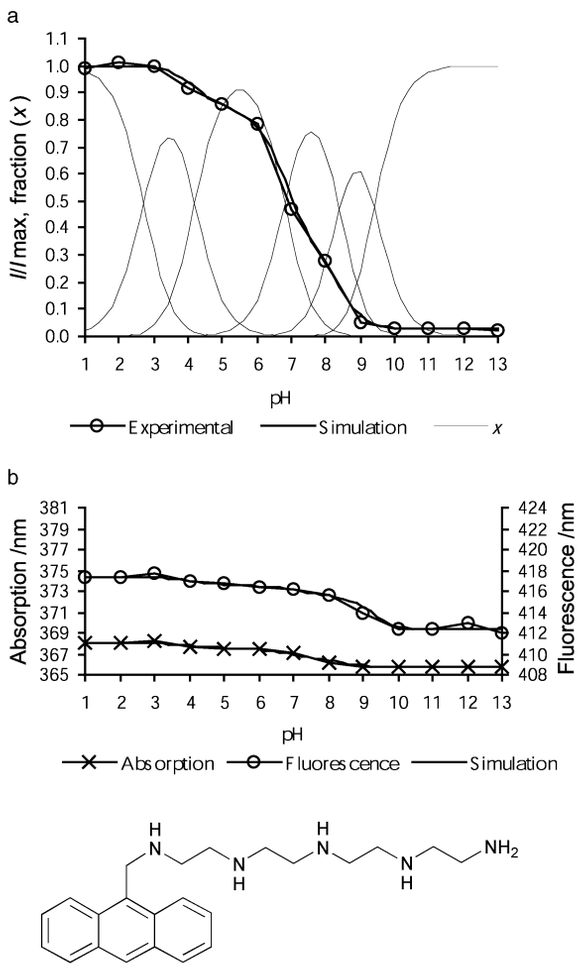

Fig. 2 Pentaamine **6**, pK_A 2.7; 4.2; 6.8; 8.4; 9.4. **a** Fluorescence intensity–pH profiles and fraction–pH profiles. Numerical simulation: $I = x(H_5A^{5+}) + x(H_4A^{4+}) + 0.84x(H_3A^{3+}) + 0.33x(H_2A^{2+}) + 0.031\{x(HA^+) + x(A)\}$. **b** Absorption maxima ($S_{0,0} \longrightarrow S_{1,1}$)–pH profiles and fluorescence maxima ($S_{1,0} \longrightarrow S_{0,1}$)–pH profiles. Numerical simulation: $\lambda_{abs} = \{x(H_5A^{5+}) + x(H_4A^{4+})\} \times 368.0$ nm + $x(H_3A^{3+}) \times 367.5$ nm + $x(H_2A^{2+}) \times 366.6$ nm + $\{x(HA^+) + x(A)\} \times 365.7$ nm; $\lambda_{flu} = [\{x(H_5A^{5+}) + x(H_4A^{4+})\} \times 417.3$ nm + $0.84x(H_3A^{3+}) \times 416.5$ nm + $0.33x(H_2A^{2+}) \times 415.5$ nm + $0.031\{x(HA^+) + x(A)\} \times 412.4$ nm$]/[x(H_5A^{5+}) + x(H_4A^{4+}) + 0.84x(H_3A^{3+}) + 0.33x(H_2A^{2+}) + 0.031\{x(HA^+) + x(A)\}]$.

they all have the same fluorescence lifetime, τ_2, and the PET competes equally strongly for deactivation, and hence causes the same remaining fluorescence intensity. If the fluorescence intensity of a particular protonation step corresponds to a lifetime between τ_2 and τ_3, it is supposed that within this protonation step, there are species having the amine group closest to the anthracene moiety protonated and hence having lifetime τ_2, and species with this amine group unprotonated and hence having the lifetime τ_3 and low fluorescence intensity.

Furthermore, it is assumed that the lowest fluorescence intensity I_{min} comes from the unprotonated species and, apart from the monoamines **1** and **2**, also from some isomers of the monoprotonated forms, and that these species have the shortest lifetime τ_3 with the highest PET rates. There are up to 4-fold protonated species with isomers where the amine group closest to the anthracene moiety is not protonated, *i.e.* with the shortest lifetime τ_3 (Table 4). In Fig. 5 these relationships are outlined for diamine **3**.

As there is a red shift in the absorption spectra of the protonated species compared to the unprotonated species of approximately 2 nm and in the fluorescence spectra of approximately 5 nm, there are two further pH dependent quantities. These effects are small, but significant. Analogously to the procedure used in eqn. (8), the wavelengths at the absorption and fluorescence maxima *versus* pH were simulated. The results of these simulations are displayed together with the experimental data in Fig. 1b to 4b. Thus, the above results are corroborated. In some cases the fluorescence wavelength of the inflection points are shifted to higher pH values: at a specific pK_A value, the fractions of the two forms are equal, and they

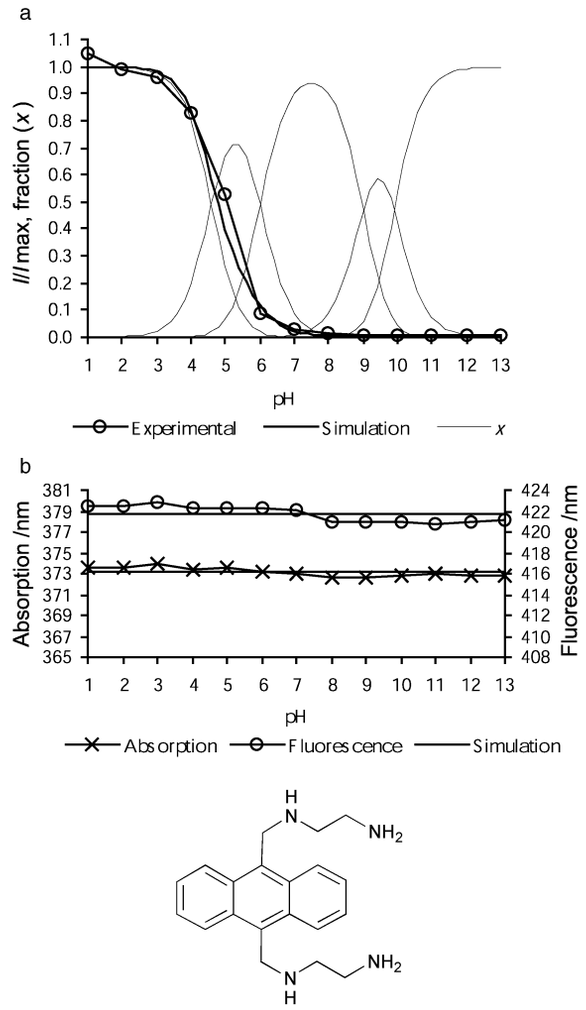

Fig. 3 Bis-diamine **11**, pK_A 4.6; 6.0; 9.0; 9.9. **a** Fluorescence intensity–pH profiles and fraction–pH profiles. Numerical simulation: $I = x(H_4A^{4+}) + 0.20x(H_3A^{3+}) + 0.0055\{x(H_2A^{2+}) + x(HA^+) + x(A)\}$. **b** Absorption maximum ($S_{0,0} \longrightarrow S_{1,1}$). Simulation: λ_{abs} = 373.2 nm; fluorescence maximum ($S_{1,0} \longrightarrow S_{0,1}$). Simulation: λ_{flu} = 421.7 nm.

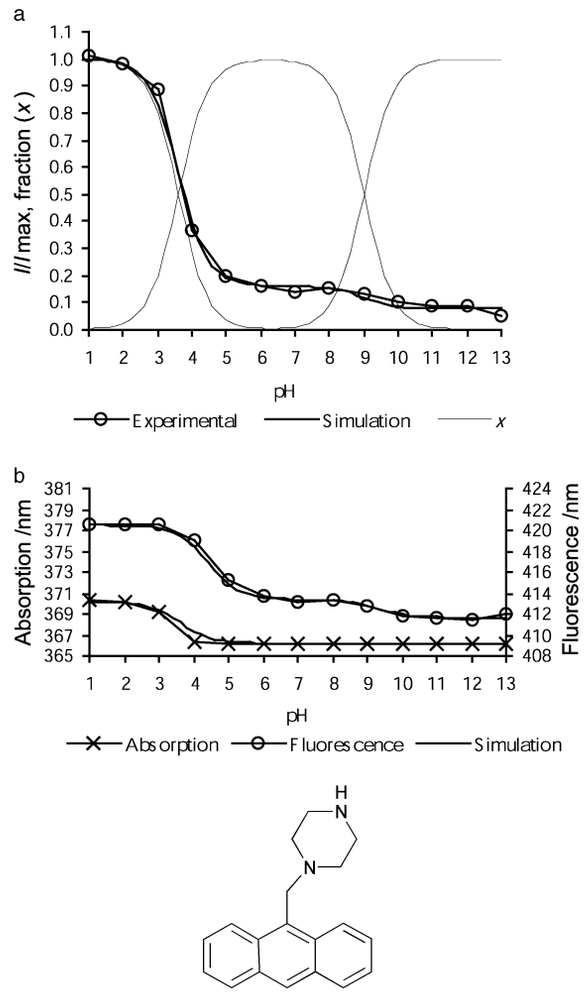

Fig. 4 Cyclic diamine **14**, pK_A 3.6; 9.0. **a** Fluorescence intensity–pH profiles and fraction–pH profiles. Numerical simulation: $I = x(H_2A^{2+}) + 0.16x(HA^+) + 0.078x(A)$. **b** Absorption maxima ($S_{0,0} \longrightarrow S_{1,1}$)–pH profiles and fluorescence maxima ($S_{1,0} \longrightarrow S_{0,1}$)–pH profiles. Numerical simulation: $\lambda_{abs} = x(H_2A^{2+}) \times 370.2$ nm + $\{x(HA^+) + x(A)\} \times 366.2$ nm; $\lambda_{flu} = \{x(H_2A^{2+}) \times 420.5$ nm + $0.16x(HA^+) \times 413.4$ nm + $0.078x(A) \times 411.7$ nm$\}/\{x(H_2A^{2+}) + 0.16x(HA^+) + 0.078x(A)\}$.

absorb equally strongly, but the less protonated form fluoresces more weakly, and thus has a smaller influence on the position of the maximum than the other form. For the 9,10-disubstituted anthracenes **11** to **13**, essentially no wavelength shift, neither in absorption nor in emission, was observed.

Discussion

pK_A values

Reported pK_A values of the investigated anthrylmethylamines are scarce. Therefore, the pK_A values of the respective methylamines and amines are also taken into account, and compared with the experimental pK_A values of eight of the investigated amines.[1b,d,8] Because of the steric hindrance of the bulky anthracene moiety and its electron attraction, the basicity of the amine groups is lowered, and hence the acidity of the conjugated acid increased.[1a] Czarnik reports that for the amine group closest to the anthracene moiety, the pK_A value is lowered by about 1 to 1.5 pH units compared to the methylene amine unit.[1e] We found pK_A shifts of 1.0 to 1.9. The influence on the other amine groups is much smaller.[8a]

For the diamines **3**, **7** and **14**, the pK_{A1} value shows a higher reduction than the pK_{A2} value, compared to the amine compartment.[1d,8a,c] This means, starting from the completely protonated form, the deprotonation of the stronger acidic amine group closest to the anthracene moiety is preferred. This confirms the fluorescence–pH profiles: there, 20% (**3**), 14% (**7**, Fig. 5) and 1.6% (**14**) of the monoprotonated forms are assumed not to be protonated at the amine group closest to the anthracene moiety, with the short lifetime τ_3 and low fluorescene intensity I_{min}. For the triamine **4** the pK_{A2} value shows the highest reduction compared to the methylene amine, and compared to the amine unit.[8d] This means, starting from the completely protonated form, the middle amine group is first deprotonated for best charge separation. In the second step, the deprotonation of the amine group closest to the anthracene moiety is preferred. This confirms the fluorescence–pH profiles, the doubly protonated form having the lifetime τ_1' and a high fluorescence intensity. For the monoprotonated form, it is assumed that 27% is protonated at the amine group closest to the anthracene moiety. For the tetraamine **10**, the pK_{A2} value shows the highest reduction compared to the amine unit.[8e]

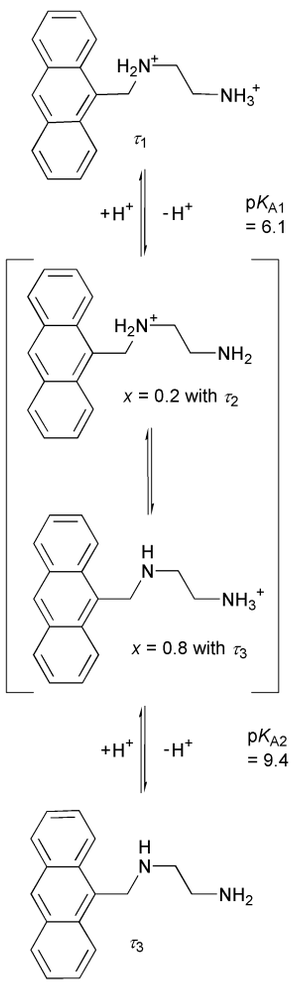

Fig. 5 Protonation equilibria of diamine **3**.

Analogously to triamine **4**, it is assumed that first the central amine group is deprotonated. In the second step, the deprotonation of the amine group closest to the anthracene moiety is preferred. This confirms the fluorescence–pH profile: the triply protonated form has the fluorescence lifetime τ_2 and an intermediate fluorescence intensity. For the doubly protonated form, it is assumed that 39% is protonated at the amine group closest to the anthracene group, with fluorescence lifetime τ_2 and an intermediate fluorescence intensity, and the remaining 61% is not protonated at the amine group closest to the anthracene group, with lifetime τ_3 and low fluorescene intensity.

Fluorescence quantum yields at low pH values

It is reported for fluorophore–spacer–ionophore systems that all absorption and emission parameters and (partially) the acid–base behaviour can be predicted from its components, except for the fluorescence quantum yield of the form without PET.[1b,3] So, for monoamine **2** in methanol : water (1 : 4 v/v) a fluorescence quantum yield of 0.69 is reported.[1b] Here, a similar value, 0.73, was determined.

Fluorescence lifetimes

The longest fluorescence lifetime of each substance is τ_1 with approximately 10 to 13 ns. These values are similar to reported fluorescence lifetimes of 9,10-disubstituted anthracenes in alcohol and significantly longer than those of reported 9-monosubstituted anthracenes in alcohol.[9] This might be caused by the long side chains and the different solvents. For the azamacrocycles **14** to **16**, the longest fluorescence lifetime τ_1 is not assigned to the completely protonated species otherwise the completely protonated species has a biexponential fluorescence decay. For this reason the fluorescence quantum yields of the azamacrocycles are smaller, although the fluorescence lifetimes τ_1 are essentially identical. This may relate to the interesting, but unexplained, finding that the maximum emission intensity of equimolar solutions of anthrylmethylazamacrocycles varies significantly.[1d]

The measured fluorescence lifetimes τ_2 are 3 to 5 ns. The corresponding fluorescence intensities can be used for the interpretation of the fluorescence–pH profiles. The only exception is the doubly protonated pentaamine **6** with a simulated fluorescence intensity corresponding to 3.9 ns, instead of the experimental fluorescence lifetime τ_2 = 2.7 ns. For the doubly protonated tetraamines **5** and **8** and the triply protonated tetramine **10**, the simulated fluorescence intensity corresponds to the fluorescence lifetime τ_2, which means that the amine group closest to the anthracene moiety is always protonated in these species (Table 4).

Surprisingly, for the 9,10-disubstituted anthracene **12**, no intermediate fluorescence lifetime τ_2 was observed. Therefore the triply protonated species was interpreted as consisting of species with the lifetime τ_1 (57%) and τ_3 (43%). A similar ratio was found for the triply protonated 9,10-disubstituted anthracene **11**, consisting of species with the lifetime τ_2 (58%) and τ_3 (42%). Also a similar ratio of species with the amine group closest to the anthracene moiety protonated (**7**: fraction 14%; **3**: 20%) was assumed for the monoprotonated species of the respective monosubstitited anthracenes **7** and **3** to fit the fluorescence–pH profiles.

Materials and methods

Potentiometric titration measurements

10 ml solution with $c = 0.001$ mol l^{-1} was titrated with sodium hydroxyde of $c = 0.1$ mol l^{-1}. The pH was measured with a glass electrode.

Chemicals

Sulfuric acid, chloroacetate, acetate, phosphate and borate buffers and sodium hydroxyde were used to buffer the solutions (pH = 1, 2, ... 13).

For each substance, an original solution with ten times the concentration of that used for measurements was prepared.

The concentrations for measurements were 10^{-5} mol l^{-1}, but 3×10^{-6} mol l^{-1} for monoamine **2** because of low solubility and 2.5×10^{-5} mol l^{-1} for the azamacrocycles **14** to **16**.

Absorption and fluorescence measurements

Absorption spectra were obtained with a Varian Cary 4E photometer. Fluorescence measurements were performed with a Perkin-Elmer LS50B fluorimeter. The excitation slit was 15 nm, as wide as possible, to compensate for spectral shifts with protonation.

Fluorescence lifetime measurements

An Edinburgh Instruments LTD nanosecond flashlamp 199F, filled with 0.5 bar D_2 or with 0.5 bar N_2, was used. The optical unit was an IBH Consultants LTD 5000U fluorescence lifetime spectrometer. A Mullard XP 2254B Photomultiplier, Ortec electronics and a Viking Instruments Inc. Norland 5000 MultiChannel Analyser System were used.

References

1 (*a*) R. A. Bissell, E. Calle, A. P. de Silva, H. Q. N. Gunaratne, J. L. Habib-Jiwan, S. L. A. Peiris, R. A. D. D. Rupasinghe, T. K. Shantha, D. Samarasinghe, K. R. A. S. Sandanayake and J. Ph.

Soumillon, *J. Chem. Soc., Perkin Trans. 2*, 1992, 1559–1564; (*b*) R. A. Bissell, A. P. de Silva, H. Q. N. Gunaratne, P. L. M. Lynch, G. E. M. Maguire and K. R. A. S. Sandanayake, *Chem. Soc. Rev.*, 1992, 187–195; (*c*) B. K. Seliger, *Aust. J. Chem.*, 1977, **30**, 2087–2090; (*d*) E. U. Akkaya, M. E. Huston and A. W. Czarnik, *J. Am. Chem. Soc.*, 1990, **112**, 3590–3593; (*e*) A. W. Czarnik, *Acc. Chem. Res.*, 1994, **27**, 302–308; (*f*) A. P. de Silva and R. A. D. D. Rupasinghe, *J. Chem. Soc., Chem. Commun.*, 1985, 1669–1670.

2 (*a*) M. E. Huston, K. W. Haider and A. W. Czarnik, *J. Am. Chem. Soc.*, 1988, **110**, 4460–4462; (*b*) A. P. de Silva and S. A. de Silva, *J. Chem. Soc., Chem. Commun.*, 1986, 1709–1710; (*c*) L. Fabbrizzi, M. Liccelli, P. Pallavicini, A. Perotti and D. Sacchi, *Angew. Chem.*, 1994, **106**(19), 2051–2053; (*d*) A. P. de Silva and H. Q. N. Gunaratne, *J. Chem. Soc., Chem. Commun.*, 1990, 186–188; (*e*) A. P. de Silva and K. R. A. S. Sandanayake, *J. Chem. Soc., Chem. Commun.*, 1989, 1183–1185; (*f*) M. E. Huston, C. Engleman and A. W. Czarnik, *J. Am. Chem. Soc.*, 1990, **112**, 7054–7056; (*g*) M. E. Huston, E. U. Akkaya and A. W. Czarnik, *J. Am. Chem. Soc.*, 1989, **111**, 8735–8737; (*h*) L. Fabbrizzi, M. Liccelli, P. Pallavicini, A. Perotti, A. Taglietti and D. Sacchi, *Chem. Eur. J.*, 1996, **2**(1), 75–82; (*i*) J. P. Konopelski, F. Kotzyba-Hibert, J. M. Lehn, J. P. Desvergne, F. Fages, A. Castellan and H. Bouas-Laurent, *J. Chem. Soc., Chem. Commun.*, 1985, 433–436; (*j*) F. Fages, J. P. Desvergne, H. Bouas-Laurent, P. Marsau, J. M. Lehn, F. Kotzyba-Hibert, A. M. A. Gary and M. Al-Joubbeh, *J. Am. Chem. Soc.*, 1989, **111**, 8672–8680.

3 A. P. de Silva, S. A. de Silva, A. S. Dissanayake and K. R. A. S. Sandanayake, *J. Chem. Soc., Chem. Commun.*, 1989, 1054–1056.

4 A. P. de Silva, H. Q. N. Gunaratne, P. L. M. Lynch, A. J. Patty and G. L. Spence, *J. Chem. Soc., Perkin Trans. 2*, 1993, 1611–1616.

5 C. Bliefert, *pH-Wert-Berechnungen*, 1st edn., Verlag Chemie, Weinheim, 1978.

6 A. P. de Silva and K. R. A. S. Sandanayake, *Tetrahedron Lett.*, 1991, **32**(3), 421–424.

7 C. A. Parker, *Photoluminescence of Solutions*, 1st edn., Elsevier Publishing Company, Amsterdam, 1968.

8 (*a*) V. Frenna and N. Vivona, *J. Chem. Soc., Perkin Trans. 2*, 1985, 1865–1868; (*b*) A. Streitwieser and C. H. Heathcock, *Introduction to Organic Chemistry*, 1st edn., Macmillan Publishing Co. Inc., New York, 1976; (*c*) H. Beyer and W. Walter, *Lehrbuch der Organischen Chemie*; 20th edn., S. Hirzel ed., Verlag, Stuttgart, 1984; (*d*) J. Yperman, J. Mullens, J.-P. Francois and L. C. Van Poucke, *J. Phys. Chem.*, 1982, **86**, 298–303; (*e*) A. Dei, P. Paoletti and A. Vacca, *Inorg. Chem.*, 1968, **7**(5), 865–870.

9 J. B. Birks, *Photophysics of Aromatic Molecules*; 1st edn., Wiley-Interscience, London, 1970.